

Multivariate Realized Volatility Forecasting with Graph Neural Network

Qinkai Chen^{†‡} Christian-Yann Robert[§]

[†]Ecole Polytechnique, Palaiseau, France

[‡]Exoduspoint Capital Management France, Paris, France

[§]ENSAE Paris, Palaiseau, France

qinkai.chen@polytechnique.edu

christian-yann.robert@ensae.fr

Abstract

The existing publications demonstrate that the limit order book data is useful in predicting short-term volatility in stock markets. Since stocks are not independent, changes on one stock can also impact other related stocks. In this paper, we are interested in forecasting short-term realized volatility in a multivariate approach based on limit order book data and relational data. To achieve this goal, we introduce Graph Transformer Network for Volatility Forecasting. The model allows to combine limit order book features and an unlimited number of temporal and cross-sectional relations from different sources. Through experiments based on about 500 stocks from S&P 500 index, we find a better performance for our model than for other benchmarks.

1 Introduction

Volatility is an important quantity in finance, it evaluates the price fluctuation and represents the risk level of an asset. It is one of the most important indicators used in risk management and equity derivatives pricing. Although the volatility is not observable, Andersen and Bollerslev (1998) show that realized volatility is a good estimator of volatility. Forecasting realized volatility has therefore attracted the attention of various researchers.

Brailsford and Faff (1996) propose using GARCH (Generalized AutoRegressive Conditional Heteroskedasticity) models to forecast realized volatilities based on daily prices. Gatheral and Oomen (2010) introduce several simple volatility estimators based on Limit Order Book

(LOB) data, showing that the use of LOB data can lead to better predicting results. More recently, Rahimikia and Poon (2020b) and Zhang and Rosenbaum (2020) use machine learning techniques such as Recurrent Neural Network (RNN) to improve such predictions.

The aforementioned literatures adopt a univariate approach in this task, which means that the model only considers one outcome for one stock at the same time, instead of jointly considering the situations of all stocks, although the asset returns on the financial markets can be highly correlated (Campbell et al., 1993). Andersen et al. (2005) propose linear multivariate volatility forecasting methods based on daily price data to take into account this correlation, while Bucci (2020) further uses neural networks to forecast realized volatility covariance matrix non-linearly. Bollerslev et al. (2019) first propose a parametric multivariate model based on LOB data using covolatility and covariance matrices. More recently, a Kaggle multivariate realized volatility prediction competition¹ was sponsored by Optiver to challenge data scientists to propose new multivariate forecasting methods.

Compared with the univariate approach, multivariate models can capture the relations among observations. Most recently, Graph Neural Networks (GNN) (Bruna et al., 2013) are proposed to integrate such relationship into the commonly used non-linear neural networks. This approach achieves significant success in multiple applications, such as traffic flow prediction (Li et al., 2017), recommender systems (Berg et al., 2017) and stock movement prediction (Sawhney et al., 2020; Chen and Robert, 2021). To the best of our knowledge, no graph-based structure for volatility forecasting has been proposed in the literatures.

The authors would like to thank Mathieu Rosenbaum from Ecole Polytechnique for his valuable guidance and advice during this work. The authors also would like to express our gratitude to Kaggle users AlexiosLyon and Max2020 for their posts and discussions. The authors also appreciate the insightful discussions with Jianfei Zhang.

¹<https://www.kaggle.com/c/optiver-realized-volatility-prediction>

Hence, to further improve the volatility forecasting performance, inspired by previous researches (Sec. 2), the Kaggle competition and our real-life use cases, we build a multivariate volatility forecasting model (Sec. 3) based on Graph Neural Network: Graph Transformer Network for Volatility Forecasting (GTN-VF). This model predicts the short-term volatilities from LOB data and both cross-sectional and temporal relationships from different sources (Sec. 4). With various experiments on about 500 stocks from the S&P 500 index, we demonstrate that GTN-VF outperforms other baseline models with a significant margin on different forecasting horizons (Sec. 5).

2 Related Work

2.1 Volatility Forecasting

As introduced in Section 1, there are two types of volatility forecasting models: univariate models and multivariate models.

In univariate approaches, researchers can design intuitive estimators (Zhou, 1996; Zhang, 2006), without considering relations among observations. More commonly, researchers adopt time-series methods to model the time dependence while ignoring the cross-sectional relations and calibrating one set of parameters for each asset. For example, Brailsford and Faff (1996) propose GARCH models, Sirignano and Cont (2019) use RNN models with Long Short-Term Memory (LSTM) and Ramos-Pérez et al. (2021) adopt a Transformer structure (Vaswani et al., 2017).

Multivariate models add cross-sectional relationships and achieve better results. For example, Kwan et al. (2005) introduce multivariate threshold GARCH model and Bollerslev et al. (2019) propose a multivariate statistical estimator based on co-volatility matrices. It is worth noting that all models above only use asset covariance as the source to build the relationship while ignoring the intrinsic relations between the companies that issue the stocks.

2.2 Graph Neural Network

A graph is composed of nodes and edges, where a node represents an instance in the network and an edge denotes the relationship between two instances. It is an intuitive structure to describe the relational information. Recently, many researches focus on generalizing neural networks on graph

structure to capture non-linear interactions among the nodes.

Bruna et al. (2013) first generalize the Convolutional Neural Network (CNN) on graph-based data, while (Kipf and Welling, 2016) propose Graph Convolutional Network (GCN) and Deferrard et al. (2016) introduce ChebNet, both of which have reduced network complexity and better predictive accuracy.

However, the aforementioned models are required to load all the graph data into the memory at the same time, making training larger relation networks impossible. Gilmer et al. (2017) state that Graph Neural Networks are essentially message passing algorithms. It means that the model makes decision not only based on one node’s observation, but also the information passed from all other related nodes defined in the format of a graph. Based on this generalization, Hamilton et al. (2017) propose GraphSAGE which allows batch training on graph data.

Shi et al. (2020) further show that using a Transformer-like operator to aggregate node features and the neighbor nodes’ features gives a better performance than a simple average such as GraphSAGE or an attention mechanism such as Graph Attention Network (Veličković et al., 2017).

To close the gap in the researches, we propose GTN-VF, which adopts the state-of-the-art Graph Neural Networks to model the relationships. In addition, GTN-VF allows to integrate an unlimited number of relational information, including both widely used covariance and other external relations such as sector and supply chain, which were rarely used in previous researches.

3 Problem Formulation

We formulate this multivariate volatility forecasting problem as a regression task. The goal is to predict the realized volatility vector over the next ΔT seconds at a given time t with all previously available data.

We first define the return of stock s at time t as

$$r_{s,t} = \log\left(\frac{P_{s,t}}{P_{s,t-1}}\right) \quad (1)$$

where $P_{s,t}$ is the last trade price of s at t .

We then use $RV_{s,t,\Delta T}$ to denote the realized volatility for stock s between t and $t + \Delta T$, it is

defined as:

$$RV_{s,t,\Delta T} = \sqrt{\sum_{i=t}^{t+\Delta T} r_{s,i}^2} \quad (2)$$

Previous researches (Malec, 2016; Rahimikia and Poon, 2020a,b) usually calibrate one model for each stock. This prediction model f_s for stock s can be written as:

$$\widehat{RV}_{s,t,\Delta T} = f_s([D_{s,t_1}, \dots, D_{s,t_m}], \theta) \quad (3)$$

where $D_{s,t}$ denotes the limit order book data related to stock s between t and $t - \Delta T'$, and $t_1 < \dots < t_m < t$. $\Delta T'$ is a parameter denoting the backward window used to build features for t , while θ represents the model parameters.

However, as stated in Section 1, the realized volatilities of the stocks are related through their LOBs. We want to consider this effect in our model and we write our prediction model g_0 as:

$$\widehat{RV}_{s,t,\Delta T} = g_0\left(\begin{bmatrix} D_{s_1,t_1} & \dots & D_{s_1,t_m} \\ \dots & \dots & \dots \\ D_{s_n,t_1} & \dots & D_{s_n,t_m} \end{bmatrix}, \mathcal{G}_s, \theta\right) \quad (4)$$

where \mathcal{G}_s is the relationship of stock s with all other stocks s_1, \dots, s_n . It means that our model jointly considers all the features from all other stocks when predicting realized volatility for stock s and its relationship with other stocks, instead of only taking its own features into account.

In addition to the relationship among stocks, we can also consider the relationship among the timestamps we predict. For example, at time t , we can check whether the behaviors of the stocks are similar to their behaviors at previous timestamps. We use \mathcal{G}_t to denote this temporal relationship. Our prediction model g is finally written as:

$$\widehat{RV}_{s,t,\Delta T} = g\left(\begin{bmatrix} D_{s_1,t_1} & \dots & D_{s_1,t_m} \\ \dots & \dots & \dots \\ D_{s_n,t_1} & \dots & D_{s_n,t_m} \end{bmatrix}, \mathcal{G}_s, \mathcal{G}_t, \theta\right) \quad (5)$$

4 Graph Transformer Network for Realized Volatility Forecasting

Our model consists of two main components: a LOB data encoder and a Graph Transformer Network. The LOB data encoder transforms numerical LOB data into multiple features. It also transforms categorical information, such as the stock

ticker, into a fixed-dimension embedding. It finally concatenates the numerical features and the embedding for categorical features as the node feature.

The Graph Transformer Network then takes all the node features and the pre-defined relationship information as input. After training, it will give each node a new meaningful embedding which contains information from both LOB data and relational data. With a fully connected layer, we can get the final prediction of realized volatility for this node.

An illustration of the whole structure is shown in Figure 1.

4.1 LOB data encoder

We first divide our LOB data $D_{s,t}$ into two parts: numerical data $D_{s,t}^{num}$ and categorical data $D_{s,t}^{cat}$. For numerical data, we can define different functions to aggregate them into numerical values. Suppose that we have k_{num} such functions $f_1, \dots, f_{k_{num}}$, we get k_{num} features and we put them into a single vector $F_{s,t}^{num}$ where

$$F_{s,t}^{num} = [f_1(D_{s,t}^{num}), \dots, f_{k_{num}}(D_{s,t}^{num})]^T \quad (6)$$

$F_{s,t}^{k_{num}}$ is therefore a vector of size $k_{num} \times 1$.

Following Kercheval and Zhang (2015); Bissoondoyal-Bheenick et al. (2019); Mäkinen et al. (2019), we define a similar set of numerical features. We also add some other features which are suitable for our dataset. We show the detailed list of features we use in our experiments in Appendix A.

For other categorical features, such as stock ticker, we simply adopt an embedding layer to transform them into a fixed-dimension vector $F_{s,t}^{cat}$. This vector is of size $k_{cat} \times 1$ where k_{cat} is the embedding dimension we can choose.

We then concatenate these two vectors into one vector $F_{s,t} \in \mathbb{R}^{k \times 1}$, where $k = k_{num} + k_{cat}$. This operation is written as

$$F_{s,t} = F_{s,t}^{num} \oplus F_{s,t}^{cat} \quad (7)$$

where \oplus denotes the concatenation operation.

4.2 Graph Transformer Network

As stated in Section 2.2, Graph Transformer operator shows a better performance compared with other structures, we use it to build our network in this study.

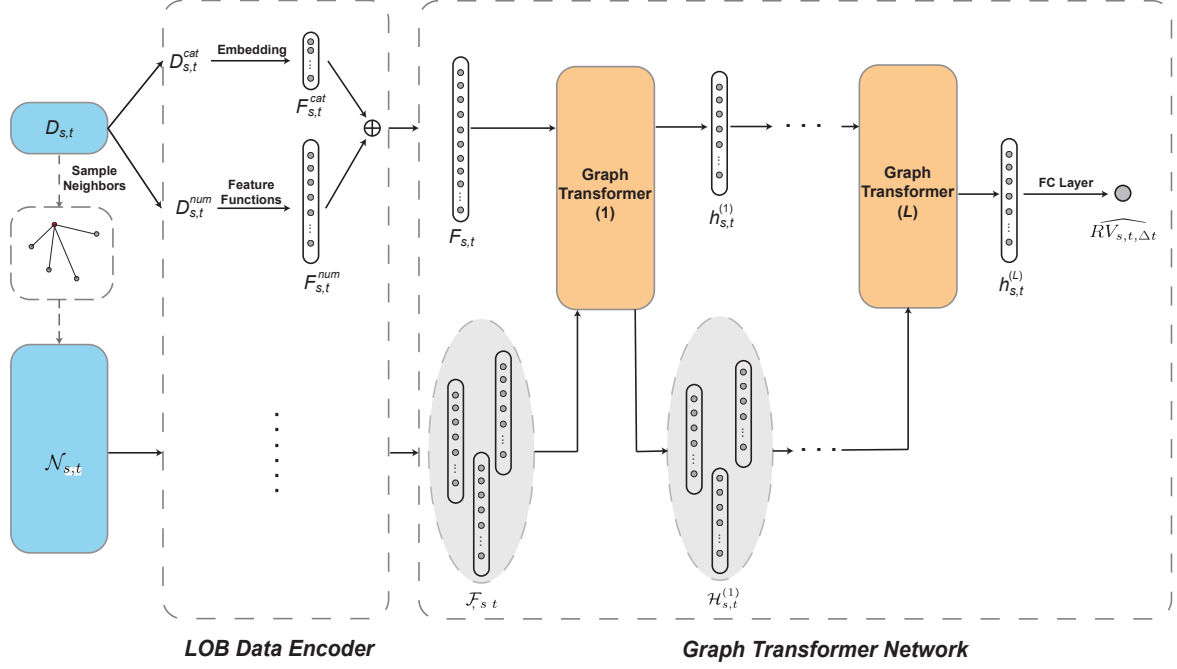


Figure 1: Structure of our Graph Transformer Network for Volatility Forecasting. This illustration shows the prediction process for one node $node_{s,t}$. The LOB data encoder first transforms its LOB data into a fixed-dimension node feature $F_{s,t}$. GTN then takes this node feature and all the features from all other nodes connected with this node ($\mathcal{F}_{s,t}$). After L Graph Transformer operations, we get the node embedding $h_{s,t}^{(L)}$ as output. We then use a fully connected layer to transform this node embedding into our final prediction $\widehat{RV}_{s,t,\Delta T}$.

We first build a graph with $m \times n$ nodes where m is the number of timestamps and n is the number of stocks. Each node $node_{s,t}$ represents the situation of stock s at time t . Its initial node feature is $F_{s,t}$ (Equation 7) encoded by LOB data encoder. From the relationship \mathcal{G}_s and \mathcal{G}_t , we can find all other nodes connected with $node_{s,t}$. We use $\mathcal{N}_{s,t}$ to denote all the connected nodes. For each stock s at time t , the model takes both its own LOB features and the LOB features from other related pairs of (s, t) into account. It then forecasts the realized volatility based on both self node features and neighbor node features, instead of the traditional approach which considers only self node features.

The Graph Transformer operator for the l -th layer with C heads is written as:

$$\widehat{h}_{s,t,c}^{(l+1)} = W_{1,c}h_{s,t}^{(l)} + \sum_{node_{i,j} \in \mathcal{N}_{s,t}} \alpha_{i,j,c} W_{2,c}h_{i,j}^{(l)} \quad (8)$$

$$h_{s,t}^{(l+1)} = \sigma(\oplus_{c=1}^C \widehat{h}_{s,t,c}^{(l+1)}) \quad (9)$$

Equation 8 first calculates the output vector $\widehat{h}_{s,t,c}^{(l+1)}$ for one single head c , in which $h_{i,j}^{(l)} \in \mathbb{R}^{d_l \times 1}$ is the l -th layer hidden node embedding for

$node_{i,j}$, $W_{1,c}, W_{2,c} \in (\mathbb{R}^{\widehat{d}_{l+1} \times d_l})^2$ are trainable parameters. $\alpha_{i,j,c}$ are attention coefficients associated with $node_{i,j}$ for head c . It is calculated via dot product attention (Bahdanau et al., 2014) by

$$\alpha_{i,j,c} = softmax\left(\frac{(W_{3,c}h_{s,t}^{(l)})^\top (W_{4,c}h_{i,j}^{(l)})}{\sqrt{d_l}}\right) \quad (10)$$

where $W_{3,c}$ and $W_{4,c}$ are both trainable parameters of size $\widehat{d}_{l+1} \times d_l$.

We then use Equation 9 to aggregate the output from all heads into a final output vector $h_{s,t}^{(l+1)}$ for the l -th layer. It is then used as the input for the $(l+1)$ -th layer. In this equation, \oplus denotes the concatenation operation and σ is an activation function such as ReLU (Glorot et al., 2011). We show the structure of this operator in Figure 2.

We can then accumulate multiple layers of this structure to better retrieve information. Suppose that our Graph Transformer Network (GTN) has L layers in total, for each node, its initial node features $h_{s,t}^{(0)} = F_{s,t}$ will be transformed into a node embedding $h_{s,t}^{(L)} \in \mathbb{R}^{d_L \times 1}$. We then use a fully-connected layer to get the final predictions of realized volatility from the node embeddings. This

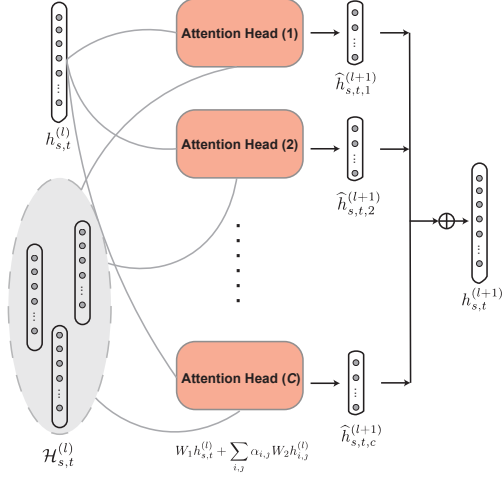


Figure 2: Illustration of Graph Transformer operator. $\mathcal{H}_{s,t}^l$ represents the l -th layer hidden vectors for all the nodes in $\mathcal{N}_{s,t}$. We can then accumulate multiple layers of this structure to build a Graph Transformer Network.

operation is written as

$$\widehat{RV}_{s,t,\Delta T} = \sigma(W_0^\top h_{s,t}^{(L)}) \quad (11)$$

where $W_0 \in \mathbb{R}^{d_L \times 1}$ are trainable parameters in the fully connected layer.

We then use Root Mean Square Percentage Error (RMSPE) as our loss function to evaluate the model and propagate back into the model. It is define as

$$RMSPE = \sqrt{\frac{1}{N} \sum_{s,t} \left(\frac{\widehat{RV}_{s,t,\Delta T} - RV_{s,t,\Delta T}}{RV_{s,t,\Delta T} + \epsilon} \right)^2} \quad (12)$$

where N is the total number of nodes in the graph and ϵ is a small constant to avoid overflow.

We use RMSPE instead of the standard Mean Square Error (MSE) because the volatilities of different stocks are intrinsically different. For example, more liquid stocks are usually more volatile than less liquid stocks (Domowitz et al., 2001). The RMSPE loss function helps normalize the difference among stocks to make sure that the model has a similar effect on all stocks.

5 Experiments

5.1 LOB data

We use NYSE daily TAQ data² as our limit order book data. The data contains all the quotes (only first limit, i.e., best bid and best ask) and trades

²<https://www.nyse.com/market-data/historical/daily-taq>

happening in the US stock exchanges. We select the entries concerning all the stocks included in the S&P 500 index³ as our universe. Compared with other researches (5 stocks in Mäkinen et al. (2019), 23 stocks in Rahimikia and Poon (2020b)), this large selection of around 500 stocks also covers some less liquid stocks. We will show that it is more difficult to have a good prediction on less liquid stocks in Section 5.5.1.

Data Sampling

Following Barndorff-Nielsen et al. (2009); Rahimikia and Poon (2020a), we first sample the data with a fixed frequency T_f . Since we focus on short-term volatility forecasting in this paper, we use a *one second* sampling frequency instead of 5 minutes used by Rahimikia and Poon (2020a) to forecast daily volatility. Our sampling strategy is as follows:

- For quote data, we snapshot the best ask price (P_a^1), best bid price (P_b^1), best ask size (V_a^1) and best bid size (V_b^1) for each stock at the end of each second.
- For trade data, we aggregate all the trades for each stock during each second. We record the number of trades (N_t), the total number of shares traded (V_t) and the volume weighted average price (P_t)⁴ of all trades.

An example of sampled quote and trade data is shown in Table 1.

Data Bucket

As introduced in Section 3, our goal is to forecast the realized volatility ΔT seconds after a given timestamp t based on the features built from a backward window of $\Delta T'$ seconds.

Hence, we need to build buckets which have the length of $\Delta T + \Delta T'$ seconds between $t - \Delta T'$ and $t + \Delta T$. In each bucket, we only use the returns between t and $t + \Delta T$ to calculate our target $RV_{s,t,\Delta T}$, we use both returns and other information from LOBs between $t - \Delta T'$ and t to build a set of features with LOB data encoder.

In our experiments on US stocks, we create 6 buckets for each stock each day. We select 10:00,

³<https://www.spglobal.com/spdji/en/indices/equity/sp-500/#overview>

⁴ $P_t = \frac{\sum_i^{N_t} P_i V_i}{\sum_i^{N_t} V_i}$ where P_i is the price for trade i and V_i is the number of shares traded. N_t is the total number of trades recorded during second t .

Date	Symbol	seconds	P_b^1	V_b^1	P_a^1	V_a^1
1/3/2017	A	0	45.92	1	46.09	1
1/3/2017	A	1	45.92	3	46	2
1/3/2017	A	2	45.92	2	46	2
1/3/2017	A	5	45.92	2	46	1
1/3/2017	A	6	45.94	1	46.05	3

(a) sampled quote data

Date	Symbol	seconds	N_t	V_t	P_t
1/3/2017	A	0	8	1500	45.802
1/3/2017	A	1	7	24959	45.94963
1/3/2017	A	2	1	300	45.96
1/3/2017	A	3	1	100	45.9544
1/3/2017	A	5	7	916	45.97817

(b) sampled trade data

Table 1: An example of sampled quote and trade data for stock A on Jan. 3rd, 2017. In addition to the previously defined LOB fields, we also have *Date*, *Symbol* and *seconds*. The *seconds* field signifies the number of seconds after the market open. We note that the *seconds* are not continuous. This is because there are occasions that there is no update in the LOB in that second. For quote data it implies that the quote is the same as the last second, for trade data it implies that there is no trade in that second.

11:00, 12:00, 13:00, 14:00 and 15:00 EST as 6 different t . For the sake of simplicity, we use $\Delta T = \Delta T'$. We use three different ΔT of 600 seconds, 1200 seconds and 1800 seconds to show that our model is robust to this choice and is capable of forecasting volatility on different horizons. This choice also ensures that there is no overlap between buckets to avoid information leakage. The detailed experiment results are shown in Section 5.4.

Data Split

We split our LOB data into 3 parts: train, validation and test. We ensure that the validation set and the test set are no earlier than the training set to avoid backward looking. We also remove the buckets where there are no quotes or trades during ΔT . Detailed statistics of our dataset are shown in Table 2.

	train	val	test
start	Jan-17	Jan-20	Jan-21
end	Dec-19	Dec-20	Oct-21
# time	4,464	1,505	1,236
# stock	494	494	494
# bucket	2,141,108	743,068	607,770
proportion	61%	21%	18%

Table 2: The statistics of the LOB data with $\Delta T = 600$.

5.2 Graph Building

As stated in Section 3, we consider both temporal (\mathcal{G}_t) and cross-sectional (\mathcal{G}_s) relationships among buckets. In this subsection, we first introduce a method to construct relations without using other data than our LOB data. We also introduce other relations we constructed with external data, for example, stock sector and supply chain data.

5.2.1 Temporal Relationship

To construct the temporal relationship among the nodes, we only use LOB data.

As introduced in Equation 6, for each $node_{s,t}$, we can calculate k_{num} features. Suppose that $f_{s,t}^i$ is the i -th feature for stock s at time t . For each time t , we let

$$Q_t^i = ([f_{1,t}^i, \dots, f_{n,t}^i])^\top \quad (13)$$

where $Q_t^i \in \mathbb{R}^{n \times 1}$ represents the feature i of all stocks at time t .

Given a time t_0 , we calculate the RMSPE (Equation 12) of Q^i between t_0 and all other t . We then choose the K -smallest RMSPE to form K pairs of times, represented by $\mathcal{G}_{t_0} = [(t_0, t_1), \dots, (t_0, t_K)]$. Then for each such pair (t_i, t_j) , we connect the two nodes where s is the same and the time is t_i and t_j respectively. This can be written as:

$$\forall (t_i, t_j) \in \mathcal{G}_{t_0}, \forall k \in [1, n], \quad \text{connect } node_{s_k, t_i} \text{ and } node_{s_k, t_j} \quad (14)$$

After this operation, we get $K \times n$ single-directed edges in the graph for t_0 . We then repeat the same process for all t , and get $K \times n \times m$ edges in total.

In our study, we use two features to get $2 \times K \times n \times m$ edges in the graph, namely, the average quote WAP⁵ for the first 100 seconds and the average quote WAP for the last 100 seconds in the bucket.

5.2.2 Cross-sectional Relationship

Unlike times, there are intrinsic relations among stocks since each stock represents a company in the real life. Hence, in addition to building relationship based on LOB features, we can also build the cross-sectional graph with external data.

Feature Correlation

⁵Weighted Average Price, defined as $\frac{P_b^1 V_a^1 + P_a^1 V_b^1}{V_a^1 + V_b^1}$.

Using the same idea introduced in 5.2.1, we first build

$$Q_s^i = ([f_{s,1}^i, \dots, f_{s,m}^i])^\top \quad (15)$$

$Q_s^i \in \mathbb{R}^{m \times 1}$ represents the feature i of stock s at t .

We then build the edges for s_0 with

$$\forall (s_i, s_j) \in \mathcal{G}_{s_0}, \forall k \in [1, m], \text{ connect } node_{s_i, t_k} \text{ and } node_{s_j, t_k} \quad (16)$$

with $\mathcal{G}_{s_0} = [(s_0, s_1), \dots, (s_0, s_{K'})]$ denoting the stock pairs which are among the K' -smallest feature RMSPE for stock s_0 .

We repeat the same process for all stocks and we use the same features as in 5.2.1 to build another $2 \times K' \times n \times m$ edges.

Stock Sector

In finance, each company is classified into a specific sector with Global Industry Classification Standard⁶ (GICS). It is shown that the performances of stocks in the same sector are often correlated (Vardharaj and Fabozzi, 2007). Hence, we simply connect the times of a pair of stocks if they belong to the same sector. This is written as:

$$\begin{aligned} &\forall E_{sec}, \forall s_i \in E_{sec}, \forall s_j \in E_{sec} \text{ and } s_j \neq s_i, \\ &\forall k \in [1, m], \text{ connect } node_{s_i, t_k} \text{ and } node_{s_j, t_k} \end{aligned} \quad (17)$$

where E_{sec} is the ensemble of all the stocks in the sector sec .

There are four granularities in GICS sector data: Sector, Industry Group, Industry, Sub-Industry. We can therefore construct four different types of edges with this GICS sector data. In our experiments, we use the Industry granularity as it gives a good performance with a reasonable number of edges. The detail of this choice is discussed in Section 5.5.3.

Supply Chain

Supply chain describes the supplier-customer relation between companies and it is proved to be useful in multiple financial tasks such as risk management (Yang et al., 2020) and performance prediction (Chen and Robert, 2021). We use the supply chain data from Factset⁷ to build this graph.

⁶<https://www.msci.com/our-solutions/indexes/gics>

⁷<https://www.factset.com/marketplace/catalog/product/factset-supply-chain-relationships>

We connect two companies if they have a supplier-customer relationship in the training period. This is described as:

$$\forall (s_i, s_j) \in \mathcal{G}_{supply}, \forall k \in [1, m] \text{ connect } node_{s_i, t_k} \text{ and } node_{s_j, t_k} \quad (18)$$

where \mathcal{G}_{supply} is the ensemble of all the supplier-customer relations among the stocks.

We show a detailed statistics of each type of relationship we built in Table 3. In addition to using these relations separately, we can also join these relations by simply putting all the edges together in the same graph. We will show that combining the edges can help improve the result in Section 5.4.

Type	Relation	# edges
Temporal	Feature Corr	8.36M
Cross-sectional	Feature Corr Sector	8.21M
	Supply Chain	47.86M
Total		76.33M

Table 3: The number of edges in each relationship we built. The total number denotes the number of all the edges combined. It is not exactly the sum of all individual edge counts since there are duplicated edges. These numbers are based on the nodes in the training set for $\Delta T = 600$.

5.3 Baseline Models

In order to prove the effectiveness of our model structure, we also include the performance of some other widely used models as our benchmarks.

- **Naïve Guess:** We simply use the realized volatility between $t - \Delta T'$ and t to predict the target. It is written as $\widehat{RV}_{s,t,\Delta T} = RV_{s,t-\Delta T',\Delta T'}$.
- **HAR-RV:** Heterogeneous AutoRegressive model of Realized Volatility. A simple but effective realized volatility prediction model proposed by Corsi (2009).
- **LightGBM:** A gradient boosting decision tree model introduced by Ke et al. (2017). It is proven to be highly effective on tabular data.

- MLP: Multi-Layer Perception network (Rumelhart et al., 1985). We build a fully connected neural network with three layers, which have 128, 64, 32 hidden units respectively.
- TabNet: A neural network proposed by Arik and Pfister (2020) which specializes in dealing with tabular data.
- Vanilla GTN-VF: Our Graph Transformer Network for Volatility Forecasting trained without any relationship information.

In addition, we show the model performance with different relations individually to demonstrate how different types of relational data help improve the result compared with Vanilla GTN-VF and other benchmarks.

5.4 Experiment Results

In our short-term realized volatility forecasting task, we use a 3-layer ($L = 3$) Graph Transformer Network with 8 heads ($C = 8$). All three layers have 128 channels ($d_1 = d_2 = d_3 = 128$). We embed our categorical features into a 32-dimension vector ($k_{cat} = 32$).

The detailed results of our experiments are shown in Table 4. We can see that our full GTN-VF model with all four types of relational information outperforms all baseline models and each type of relational information individually on all prediction horizons. The improvement is significant. In average, we gain 6% in RMSPE compared with Naïve Guess and 2% compared with the best baseline model TabNet on test set. It proves that our GTN model structure and relation building methods are effective.

In terms of individual relationship, all relations are useful since they all show improvement compared with the vanilla model. The temporal feature correlation shows the most predicting power, contributing 1.2% RMSPE gain while the Sector relation only contributes 0.7% improvement when the window is set to 600 seconds although it has the largest number of edges. This can be explained by the 'noise' included in this type of information since we need to connect every two stocks in the same sector although not all of them have significant connection. However, feature correlation only selects the two most related stocks or times, making it more discriminational when building edges. This suggests that if we have the constraint

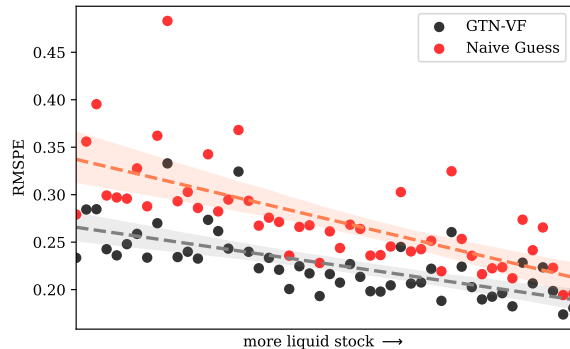


Figure 3: The relationship between stock liquidity and prediction RMSPE. The dots denote the RMSPE for the buckets and the dashed lines are the trend lines calculated with linear regression. This figure is based on test result and $\Delta T = 600$.

on the number of edges in the graph, quality is more important than quantity. On the other hand, these relations are complementary to each other, adding more relations on top of existing relations can help improve the prediction if we have enough computing power.

It is also worth noting that when we forecast the realized volatility with a longer forward looking and backward looking window, the result is better. This is simple because the same volatility jump causes more volatility changes in shorter forecasting horizon (Ma et al., 2019).

5.5 Ablation Studies

5.5.1 Prediction accuracy and stock liquidity

In general, it is more difficult to have a good prediction on less liquid stocks because there are fewer market participants for them. One sudden change in quote or trade can cause significant volatility jump, which is difficult to foresee. We analyze the result to understand where the improvement comes from.

We first split the stocks into 50 buckets according to their average daily turnover, which represents the liquidity of a stock. We calculate the RMSPE in each bucket for both Naïve Guess and GTN-VF. The result is illustrated in Figure 3.

First, we notice that more liquid stocks have smaller RMSPE for both models, which is intuitive. The prediction for the most liquid stocks is 5% better than the least liquid stocks in terms of RMSPE, which is a large margin in realized volatility forecasting. We can also see that our graph based model has more improvement on the less liquid stocks (around 8% for more liquid

Model	$\Delta T = 600$		$\Delta T = 1200$		$\Delta T = 1800$	
	val	test	val	test	val	test
Naïve Guess	0.2911	0.2834	0.2650	0.2628	0.2296	0.2364
HAR-RV	0.2684	0.2612	0.2149	0.2061	0.1968	0.1939
LightGBM	0.2583	0.2492	0.2414	0.2035	0.2349	0.1963
MLP	0.2431	0.2514	0.2200	0.2308	0.2270	0.1999
TabNet	0.2517	0.2478	0.2212	0.1996	0.2204	0.2019
Vanilla GTN-VF	0.2457	0.2498	0.2229	0.2251	0.2092	0.2160
GTN-VF Cross FC	0.2414	0.2382	0.2162	0.2196	0.2066	0.2046
GTN-VF Temp FC	0.2326	0.2358	0.1974	0.1921	0.1896	0.1853
GTN-VF Cross Sector	0.2406	0.2422	0.2067	0.2248	0.2071	0.2091
GTN-VF Cross Supply Chain	0.2430	0.2411	0.2105	0.2244	0.2057	0.2000
GTN-VF Cross FC + Temp FC	0.2326	0.2306	0.1936	0.1917	0.1848	0.1802
GTN-VF	0.2314	0.2287	0.1916	0.1892	0.1809	0.1798

Table 4: RMSPE values of all the models on both validation set and test set. In addition to the baseline models, we also include the individual performance of the GTN-VF with four relations (Table 3), i.e., Cross-sectional Feature Correlation (GTN-VF Cross FC), Temporal Feature Correlation (GTN-VF Temp FC), Cross-sectional Sector relationship (GTN-VF Sector) and Cross-sectional Supply Chain relationship (GTN-VF Cross Supply Chain). The full GTN-VF includes all four types of relations.

stocks and 2% for less liquid stocks), although it is more effective than Naïve Guess on all scenarios.

5.5.2 Prediction accuracy and node connection

We also investigate how our model performs on different nodes. We use the same approach in Section 5.5.1 by splitting nodes into buckets according to the number of edges connected to each node. We can see from Figure 4 that more connected nodes usually have better RMSPE result, with a 2% difference between the most connected and the least connected. This can be explained by the fact that more connected nodes make decision based on more information from their neighbor, while the nodes with fewer or no connections can only rely on the information from themselves. This phenomenon proves again the effectiveness of our graph based method.

5.5.3 Sector Relationship

As introduced in Section 5.2.2, there are four granularities in the GICS sector data. We run different experiments to evaluate the performance of each type of sector relationship. The result is shown in Table 5.

We observe that Industry shows the best performance with a modest number of edges. If we add more edges, such as IndustryGroup, the RMSPE decreases since the relations among stocks are less

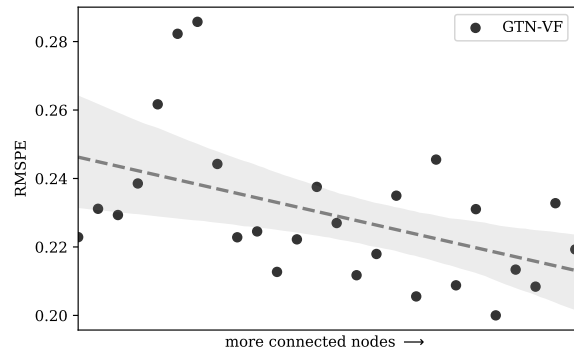


Figure 4: The relationship between node connection and RMSPE. This figure is based on test result and $\Delta T = 600$.

meaningful. For the Sector granularity, we are not even able to obtain a result since the number of edges exceeds the memory limit. Hence, in our final model combining multiple sources of relations, we choose Industry as our sector relationship.

6 Conclusion

We forecast the short-term realized volatility in a multivariate approach. We design a graph based neural network: Graph Transformer Network for Volatility Forecasting which incorporates both features from LOB data and relationship among stocks from different sources. Through extensive experiments on around 500 stocks, we

Granularity	# edges	test RMSPE
Sector	178.7M	N.A.
IndustryGroup	83.39M	0.2578
Industry	47.86M	0.2422
SubIndustry	19.88M	0.2441

Table 5: Test RMSPE with different granularities of GICS sector. The result for Sector is not available as the number of edges is too big to fit in the memory.

prove the that our method outperforms other baseline models, both univariate and multivariate. In addition, the model structure allows to combine an unlimited number of relations, the study of the effectiveness of other relational data is open for future researches.

Acknowledgments

The authors gratefully acknowledge the financial support of the Chaire *Machine Learning & Systematic Methods in Finance*.

References

- Torben G Andersen and Tim Bollerslev. 1998. Answering the skeptics: Yes, standard volatility models do provide accurate forecasts. *International economic review* pages 885–905.
- Torben G Andersen, Tim Bollerslev, Peter Christoffersen, and Francis X Diebold. 2005. Volatility forecasting.
- Sercan O Arık and Tomas Pfister. 2020. Tabnet: Attentive interpretable tabular learning. *arXiv* .
- Dzmitry Bahdanau, Kyunghyun Cho, and Yoshua Bengio. 2014. Neural machine translation by jointly learning to align and translate. *arXiv preprint arXiv:1409.0473* .
- Ole E Barndorff-Nielsen, P Reinhard Hansen, Asger Lunde, and Neil Shephard. 2009. Realized kernels in practice: Trades and quotes.
- Rianne van den Berg, Thomas N Kipf, and Max Welling. 2017. Graph convolutional matrix completion. *arXiv preprint arXiv:1706.02263* .
- Emawtee Bissoondoyal-Bheenick, Robert Brooks, and Hung Xuan Do. 2019. Asymmetric relationship between order imbalance and realized volatility: Evidence from the australian market. *International Review of Economics & Finance* 62:309–320.
- Tim Bollerslev, Nour Meddahi, and Serge Nyawa. 2019. High-dimensional multivariate realized volatility estimation. *Journal of Econometrics* 212(1):116–136.
- Timothy J Brailsford and Robert W Faff. 1996. An evaluation of volatility forecasting techniques. *Journal of Banking & Finance* 20(3):419–438.
- Joan Bruna, Wojciech Zaremba, Arthur Szlam, and Yann LeCun. 2013. Spectral networks and locally connected networks on graphs. *arXiv preprint arXiv:1312.6203* .
- Andrea Bucci. 2020. Cholesky–ann models for predicting multivariate realized volatility. *Journal of Forecasting* 39(6):865–876.
- John Y Campbell, Sanford J Grossman, and Jiang Wang. 1993. Trading volume and serial correlation in stock returns. *The Quarterly Journal of Economics* 108(4):905–939.
- Qinkai Chen and Christian-Yann Robert. 2021. Graph-based learning for stock movement prediction with textual and relational data. *arXiv preprint arXiv:2107.10941* .
- Fulvio Corsi. 2009. A simple approximate long-memory model of realized volatility. *Journal of Financial Econometrics* 7(2):174–196.
- Michaël Defferrard, Xavier Bresson, and Pierre Vandergheynst. 2016. Convolutional neural networks on graphs with fast localized spectral filtering. *Advances in neural information processing systems* 29:3844–3852.
- Ian Domowitz, Jack Glen, and Ananth Madhavan. 2001. Liquidity, volatility and equity trading costs across countries and over time. *International Finance* 4(2):221–255.
- Jim Gatheral and Roel CA Oomen. 2010. Zero-intelligence realized variance estimation. *Finance and Stochastics* 14(2):249–283.
- Justin Gilmer, Samuel S Schoenholz, Patrick F Riley, Oriol Vinyals, and George E Dahl. 2017. Neural message passing for quantum chemistry. In *International conference on machine learning*. PMLR, pages 1263–1272.
- Corrado Gini. 1921. Measurement of inequality of incomes. *The economic journal* 31(121):124–126.
- Xavier Glorot, Antoine Bordes, and Yoshua Bengio. 2011. Deep sparse rectifier neural networks. In *Proceedings of the fourteenth international conference on artificial intelligence and statistics*. JMLR Workshop and Conference Proceedings, pages 315–323.
- William L Hamilton, Rex Ying, and Jure Leskovec. 2017. Inductive representation learning on large graphs. In *Proceedings of the 31st International Conference on Neural Information Processing Systems*. pages 1025–1035.
- Guolin Ke, Qi Meng, Thomas Finley, Taifeng Wang, Wei Chen, Weidong Ma, Qiwei Ye, and Tie-Yan Liu. 2017. Lightgbm: A highly efficient gradient boosting decision tree. *Advances in neural information processing systems* 30:3146–3154.

- Alec N Kercheval and Yuan Zhang. 2015. Modelling high-frequency limit order book dynamics with support vector machines. *Quantitative Finance* 15(8):1315–1329.
- Thomas N Kipf and Max Welling. 2016. Semi-supervised classification with graph convolutional networks. *arXiv preprint arXiv:1609.02907* .
- CK Kwan, WK Li, and K Ng. 2005. A multivariate threshold garch model with time-varying correlations. *Econometric reviews* 24.
- Yaguang Li, Rose Yu, Cyrus Shahabi, and Yan Liu. 2017. Diffusion convolutional recurrent neural network: Data-driven traffic forecasting. *arXiv preprint arXiv:1707.01926* .
- Feng Ma, Yin Liao, Yaojie Zhang, and Yang Cao. 2019. Harnessing jump component for crude oil volatility forecasting in the presence of extreme shocks. *Journal of Empirical Finance* 52:40–55.
- Ymir Mäkinen, Juho Kanninen, Moncef Gabbouj, and Alexandros Iosifidis. 2019. Forecasting jump arrivals in stock prices: new attention-based network architecture using limit order book data. *Quantitative Finance* 19(12):2033–2050.
- Peter Malec. 2016. A semiparametric intraday garch model .
- Eghbal Rahimikia and Ser-Huang Poon. 2020a. Big data approach to realised volatility forecasting using har model augmented with limit order book and news. *Available at SSRN 3684040* .
- Eghbal Rahimikia and Ser-Huang Poon. 2020b. Machine learning for realised volatility forecasting. *Available at SSRN 3707796* .
- Eduardo Ramos-Pérez, Pablo J Alonso-González, and José Javier Núñez-Velázquez. 2021. Multi-transformer: A new neural network-based architecture for forecasting s&p volatility. *Mathematics* 9(15):1794.
- David E Rumelhart, Geoffrey E Hinton, and Ronald J Williams. 1985. Learning internal representations by error propagation. Technical report, California Univ San Diego La Jolla Inst for Cognitive Science.
- Ramit Sawhney, Shivam Agarwal, Arnav Wadhwa, and Rajiv Shah. 2020. Deep attentive learning for stock movement prediction from social media text and company correlations. In *Proceedings of the 2020 Conference on Empirical Methods in Natural Language Processing (EMNLP)*, pages 8415–8426.
- Yunsheng Shi, Zhengjie Huang, Shikun Feng, Hui Zhong, Wenjin Wang, and Yu Sun. 2020. Masked label prediction: Unified message passing model for semi-supervised classification. *arXiv preprint arXiv:2009.03509* .
- Justin Sirignano and Rama Cont. 2019. Universal features of price formation in financial markets: perspectives from deep learning. *Quantitative Finance* 19(9):1449–1459.
- Raman Vardharaj and Frank J Fabozzi. 2007. Sector, style, region: Explaining stock allocation performance. *Financial Analysts Journal* 63(3):59–70.
- Ashish Vaswani, Noam Shazeer, Niki Parmar, Jakob Uszkoreit, Llion Jones, Aidan N Gomez, Lukasz Kaiser, and Illia Polosukhin. 2017. Attention is all you need. *arXiv preprint arXiv:1706.03762* .
- Petar Veličković, Guillem Cucurull, Arantxa Casanova, Adriana Romero, Pietro Lio, and Yoshua Bengio. 2017. Graph attention networks. *arXiv preprint arXiv:1710.10903* .
- Shuo Yang, Zhiqiang Zhang, Jun Zhou, Yang Wang, Wang Sun, Xingyu Zhong, Yanming Fang, Quan Yu, and Yuan Qi. 2020. Financial risk analysis for smes with graph-based supply chain mining. In *IJCAI*, pages 4661–4667.
- Jianfei Zhang and Mathieu Rosenbaum. 2020. Universal volatility formation : perspective from rough volatility and deep learning. Technical report, Ecole Polytechnique.
- Lan Zhang. 2006. Efficient estimation of stochastic volatility using noisy observations: A multi-scale approach. *Bernoulli* 12(6):1019–1043.
- Bin Zhou. 1996. High-frequency data and volatility in foreign-exchange rates. *Journal of Business & Economic Statistics* 14(1):45–52.

A List of node features

We introduce the features we use in our experiments.

In each bucket, we have $\Delta T'$ lines as training data. We first calculate an indicator for each line, we then aggregate these indicators in the same bucket with an aggregation function (aggregator). In such way, we have one value per indicator per aggregator as one feature for the bucket. The full list of indicators and aggregators are listed in Table 6.

For some important indicators, we also calculate their progressive features. It means that instead of applying an aggregator on all the lines, we apply it on the lines between 0 and $\Delta T'/6$, $\Delta T'/3$, $\Delta T'/2$, $2\Delta T'/3$, $5\Delta T'/6$, $\Delta T'$. In such way, we have 6 features per indicator per aggregator for an progressive feature. This is shown in the column Progressive in Table 6.

We define our aggregation functions as follows. We use a_i to denote the i -th line in the bucket and N represents the total number of lines.

- gini coefficient (Gini, 1921)

$$\frac{\sum_i^N \sum_j^N |a_i - a_j|}{2N^2\bar{a}}$$

- percentage difference

$$\frac{\sum_i^N \mathbf{1}_{a_i \neq a_{i-1}}}{N}$$

- realized volatility (Equation 2)

$$\sqrt{\frac{1}{N} \sum_i^N a_i^2}$$

- percentage greater than mean

$$\frac{\sum_i^N \mathbf{1}_{a_i > \bar{a}}}{N}$$

- percentage greater than zero

$$\frac{\sum_i^N \mathbf{1}_{a_i > 0}}{N}$$

- median deviation

$$\text{median}(|a_i - \bar{a}|)$$

- energy

$$\frac{1}{N} \sum_i^N a_i^2$$

- InterQuartile Range (IQR)

$$Q_{75}(a) - Q_{25}(a)$$

where $Q_i(a)$ denotes the i -th percentile value for the series a .

Type	Notation	Description	Aggregators	Progressive	Count
Quote	$\frac{P_b^1 V_a^1 + P_a^1 V_b^1}{V_a^1 + V_b^1}$	WAP	mean, std, gini mean of first 100, mean of last 100	N	5
	P_a^1	Ask Price	% difference	N	1
	P_b^1	Bid Price	% difference	N	1
	$\frac{P_a^1 - P_b^1}{P_a^1 + P_b^1}$	Price Relative Spread	mean, std, gini	N	3
	$WAP - P_b^1$	WAP bid difference	mean, std, gini	N	3
	$\log(\frac{WAP_i}{WAP_{i-1}})$	Return	realized volatility	Y	6
	$\log(\frac{WAP_i}{WAP_{i-1}})^2$	Squared Return	std, gini	N	2
	$\frac{V_a^1 - V_b^1}{V_a^1 + V_b^1}$	Size Relative Spread	mean, std, gini	N	3
	V_a^1	Ask Size	% difference	N	1
	V_b^1	Bid Size	% difference	N	1
	V_a^1 / V_b^1	Normalized Ask Size	mean, std, gini	N	3
	$V_a^1 + V_b^1$	Total Size	sum, max	N	2
	$ V_a^1 - V_b^1 $	Size Imbalance	sum, max	N	2
Trade	P_t	Price	% greater than mean, % less than mean median diviation, energy, IQR	N	5
	$\log(\frac{P_{t,i}}{P_{t,i-1}})$	Return	realized volatility % greater than 0, % less than 0	Y N	6 2
	$\log(\frac{P_{t,i}}{P_{t,i-1}})^2$	Squared Return	std, gini	N	2
	V_t	Size	sum max, median diviation, energy, IQR	Y N	6 4
	t	Seconds	count	Y	6
	N_t	Order Count	sum max	Y N	6 1
	$P_t \times V_t$	Amount	sum, max	N	2
	Total				

Table 6: The list of features built from LOB data.